Thermodynamics, Transport, and Fluid Mechanics

Modelling hydrate dissociation curves in the presence of hydrate inhibitors with a modified CPA EoS.

André M. Palma, Antonio J. Queimada, and Joao A.P. Coutinho

Ind. Eng. Chem. Res., **Just Accepted Manuscript** • DOI: 10.1021/acs.iecr.9b03512 • Publication Date (Web): 20 Sep 2019

Modelling hydrate dissociation curves in the presence of hydrate inhibitors with a modified CPA EoS.

André M. Palma[1], António J. Queimada[2,*] and João A. P. Coutinho[1]

[1]CICECO, Chemistry Department, University of Aveiro, Campus de Santiago, 3810-193 Aveiro, Portugal.

[2]KBC Advanced Technologies Limited (A Yokogawa Company), 42-50 Hersham Road, Walton-on-Thames, Surrey, United Kingdom, KT12 1RZ.

*Corresponding author. E-mail address: aqueimada@kbcat.com

Abstract

A modified CPA equation of state has been applied for the description of non-inhibited hydrates. In this work, this model is applied to the description of dissociation curves of hydrates inhibited by six thermodynamic inhibitors (methanol, ethanol, MEG, DEG, TEG and glycerol), while also focusing on promoting a correct simultaneous description of SLE and VLE between the inhibitors and water. The study concern some of the most well-known hydrate formers (methane, ethane, propane, CO_2, Xe and H_2S) and mixtures of these gases. The maximum number of binary interaction parameters applied between water and the hydrate inhibitor is two, one for the physical term and one for association. A comparison between this approach and the hydrates model present on Multiflash is reported, revealing that the present approach, while less accurate than Multiflash is still able to correctly describe hydrate inhibition, VLE and LLE, while using a smaller number of parameters.

Keywords: CPA, Equation of state, Gas hydrates, Hydrate inhibition, van der Waals-Platteeuw

1. Introduction

The formation of hydrates inside pipelines or equipment are one of the major hazards that flow assurance engineers need to consider. Even with low water contents, gaseous streams rich in gases like methane or CO_2 may form this type of solid structures at low temperatures and/or high pressures. The most common method to deal with this issue is the addition of thermodynamic inhibitors, which interact with water, reducing the temperature, and/or increasing the pressure of hydrate formation.

A dedicated model is necessary to describe hydrate phases, with the most well-known models being based on the van der Waals and Platteeuw theory, [1] such as the modification proposed by Parrish and Prausnitz, [2] which is still one of the most popular. However, these models only describe the thermodynamics of the hydrate phase and a second model is necessary to describe fluid phases. In most industrial software fluid phases are either described by an equation of state or by an activity coefficient model (or both, using excess Gibbs energy mixing rules). For the case of hydrate calculations, the first is more commonly applied because of the high dissociation pressures involved. [3]

In the present study a modified CPA equation of state [4] is applied for the fluid phases. This model explicitly accounts for hydrogen bonding interactions between water and hydrate inhibitors, while keeping the simplicity of a cubic equation of state for the interactions between the different gases and the non-polar components in study. Other studies to describe hydrate inhibition with equations of state, explicitly accounting for hydrogen bonding to describe hydrate inhibition, include those of Folas *et al.* [5] and Pedrosa *et al.* [6] with CPA, Li *et al.* with SAFT, [7] Dufal *et al.* with SAFT-VR [8] and Kondori *et al.* with a combination of PC-SAFT with UNIQUAC. [9]

In this study we evaluate the performance of a modified CPA model for representing hydrate inhibition. Six hydrate inhibitors are studied (methanol, ethanol, ethylene glycol (MEG), diethylene glycol (DEG), triethylene glycol (TEG) and glycerol) in presence of single hydrate formers. The performance of the modified CPA is also investigated for some natural/sour gas mixtures in presence of inhibitors. The results here obtained are compared with those of a commercial model present in the Multiflash software [10] (6.1 version), one of the industry standards for hydrate calculations.

2. Models

The hydrate phase is described using the modified van der Waals and Platteeuw theory, [1] proposed by Parrish and Prausnitz. [2] This model is known to accurately predict hydrate dissociation temperatures for multicomponent fluids. However, there are still issues/limitations in the description obtained by this theory: The model assumes spherical symmetry; the interactions between the molecules inside each cage are not considered; and the cavities are not distorted by the presence of the guest molecule. Despite these limitations, the model is known for its accuracy and has been successfully coupled with diverse equations of state.

In this work the fluid phases are described using the modified CPA as detailed in the following section.

2.1 Modified CPA

Most of the modified CPA structure is based on the simplified CPA: [11]

$$Z = Z^{phys} + Z^{assoc} = \frac{1}{1-B\rho} - \frac{A(T)\rho}{RT(1+B\rho)} - \frac{1}{2}\left(1+\rho\frac{\delta lng}{\delta\rho}\right)\sum_i m_i(1-X_i) \quad (1)$$

A is the energy parameter ($A(T) = n^2 a(T)$), B is the co-volume ($B = nb$), ρ represents the density, g is a simplified hard-sphere radial distribution function,[11] X_{A_i} represents the mole fraction of component *i* not bonded at site A and m_i is the mole number of sites of type *i*. Equations 2-3 show the mixing rules for *a* and *b*:

$$a = \sum_i \sum_j x_i x_j a_{ij} \quad (2)$$

$$b = \sum_i x_i b_i \quad (3)$$

with:

$$a_{ij} = \sqrt{a_i a_j}(1-k_{ij}) \quad (4)$$

k_{ij} are binary interaction parameters.

The first of the four differences between the simplified CPA and the present model is in the alpha function used (based on a Mathias-Copeman polynomial). For some specific cases, like water, there are relevant changes in the description of pure component properties, when using this alpha function. [12]

$$a(T) = a_c\left(1 + T' \times c_1 + T'^2 \times c_2 + T'^3 \times c_3 + T'^4 \times c_4 + T'^5 \times c_5\right)^2 \quad (5)$$

with $T'=(1-\sqrt{T_r})$, $T_r = T/T_c$

X_i is calculated as:

$$X_i = \frac{1}{1 + g\rho\sum_j m_j X_j \Delta^{ij}} \quad (6)$$

where the association strength (Δ^{ij}) given by:

$$\Delta^{ij} = g b^{ij} \beta^{ij} \left(e^{\frac{\varepsilon^{ij}}{RT}} - 1\right) \quad (7)$$

ε^{ij} and β^{ij} are the association energy and volume for interactions between sites *i* and *j*.

The simplified radial distribution function is presented in equation 8.[11,13]

$$g(\rho) = \frac{1}{1 - 0.475 b\rho} \quad (8)$$

When two or more associative compounds are present in a mixture, CPA needs combining rules for the cross-associative parameters. CR-2[14] combining rules, as proposed by Kontogeorgis et al.[15] were applied:

$$\beta^{ij} = \sqrt{\beta^i \beta^j} \quad (9)$$

$$\varepsilon^{ij} = \frac{(\varepsilon^i + \varepsilon^j)}{2} \quad (10)$$

The second of the four changes in comparison to the simplified CPA is the correct description of the pure component critical temperatures and pressures, which imply that a_c and the co-volume (*b*) are not regressed simultaneously, but instead obtained by solving the following set of equations:

$$P_{CPA}\left(T_c^{exp}, v_c^{calc}\right) = P_c^{exp} \quad (11)$$

$$\left(\frac{\partial P}{\partial v}\right)_T \Big|_{\substack{T = T_c \\ v = v_{c,calc}}} = 0 \quad (12)$$

$$\left(\frac{\partial^2 P}{\partial v^2}\right)_T\Bigg|_{\substack{T=T_c \\ v=v_{c,\,calc}}} = 0 \tag{13}$$

where *T* is temperature, *P* is pressure, *v* is molar volume and the subscript *c* means critical. A detailed discussion on this change of parameterization can be found on previous works with this version of CPA. [4,16,17]

The third modification lies in the use of a volume shift at 0.7 T_c to fit density, instead of fitting this property directly.

$$v_t = v_0 - c_{vs} \tag{14}$$

v_t is the volume after translation, v_0 is the volume before translation and c_{vs} is the volume shift.

The fourth difference, is a consequence of the present alpha function showing inversion points on its second derivative. This fourth change introduces an extrapolation between T_c and 1.1 x T_c after which the model considers the API alpha function for the compound. [18]

The following equations were considered to optimize the values of k_{ij}.

$$OF = \sum_i^{np}\left(\frac{T_{bub}^{exp.} - T_{bub}^{calc.}}{T_{bub}^{exp.}}\right)^2 \tag{15}$$

$$OF = \sum_i^{np}\left(\frac{P_{bub}^{exp.} - P_{bub}^{calc.}}{P_{bub}^{exp.}}\right)^2 \tag{16}$$

$$OF = \sum_k^{npo}\sum_i^{nc}\left(\frac{x_{i,k}^{exp.} - x_{i,k}^{calc.}}{x_{i,k}^{exp.}}\right)^2 \tag{17}$$

where *npo* is the number of phases to optimize. As in most mixtures in study the fitting is obtained from SLE and VLE simultaneously, a weighted sum between the objective functions 17 and 15 or 16 was applied.

3. Results and discussion

Most compounds studied in this work have been previously parameterized with the modified CPA. [4,12,16,19] Exceptions to this are diethylene glycol (DEG) and triethylene glycol (TEG). The pure compound parameters for all compounds in this study are presented in Table 1. The association schemes used in this work are 4C for water, 2B for methanol and ethanol, 2x2B for the glycols and 3x2B for glycerol. The transferability approach, presented in a previous work [19] is applied for the associative parameters of the hydroxyl groups.

Table 1 – Pure component parameters used in this work

Compound	a_c *(Pa.m⁶.mol⁻²)*	*b. 10⁵ (m³.mol⁻¹)*	*c1*	*c2*	*c3*	*c4*	*c5*	*β.10²*	*ε (J.mol⁻¹)*
water	0.43	2.39	0.56	-2.54	-2.01	1.46	8.63	0.483	22013
MEG	1.72	6.87	1.10	-3.64	12.16	-37.1	42.5	0.162	24913
DEG	3.35	12.53	1.75	-9.66	43.77	-102.36	93.87	0.153	24913
TEG	5.08	17.57	2.35	-12.50	51.77	-111.32	94.40	0.113	24913
methanol	0.68	4.61	0.9	-2.47	3.26	0	0	0.465	24913
ethanol	1.13	6.40	1.04	-1.46	-0.79	3.76	0	0.162	24913

glycerol	2.59	9.11	0.45	4.16	-19.32	19.9	0	0.162	24913
methane	0.23	2.98	0.59	-1.47	9.02	-27.39	31.55		
ethane	0.57	4.51	0.71	-1.17	7.00	-20.37	22.42		
propane	0.95	6.27	0.82	-1.63	9.36	-24.39	23.68		
isobutane	1.35	8.07	0.89	-1.94	11.12	-29.03	28.57		
n-butane	1.41	8.07	0.88	-1.39	7.72	-20.51	21.48		
n-pentane	1.94	10.05	1.00	-2.08	12.24	-32.87	32.84		
N_2	0.14	2.68	0.63	-1.45	9.42	-29.74	36.21		
O_2	0.14	2.21	0.89	-1.94	11.12	-29.03	28.57		
CO_2	0.37	2.97	0.90	-1.35	5.61	0.00	0.00		
H_2S	0.46	2.99	0.72	-1.07	4.82	-8.86	5.24		
Xe	0.42	3.57	0.56	-0.51	1.60	-5.49	7.49		

CPA is usually able to describe simultaneously the freezing point depressions of water + hydrate inhibitors, as well as, hydrate dissociation curves, while using a single binary interaction parameter (a constant k_{ij}). However, using this approach leads to an incorrect description of VLE for these mixtures. The CPA model present on Multiflash is capable of describing these phase equilibria simultaneously. Nevertheless, it requires a larger number of parameters, both for the pure component and for the mixtures, than those used by the modified CPA.

In this work, for three of the six hydrate inhibitors in analysis a binary interaction parameter for the volume of association (β_{ij}) was added. For the remaining compounds, either there was a good description of the three types of phase equilibria, or there is a lack of data on one of these equilibria. Thus for these mixtures the binary interaction parameters differ from those of the previous study with water. [12] This should enable a better simultaneous description of hydrate dissociation curves and VLE.

3.1 SLE and VLE of water + hydrate inhibitors.

Before looking at the quality of the hydrate dissociation curves, it is important to look at how this approach works for both freezing point depressions and VLE. The binary interaction parameters that were used are presented in Table 2. These are different from those used in previous works, due to the simultaneous fitting to VLE and SLE equilibria. The remaining binary interaction parameters were presented in previous works [4,12,16,19,20].

Table 2 – binary interaction parameters between water and the hydrate inhibitors

Inhibitor	k_{ij}	$\beta_{ij} \cdot 10^2$
methanol	-0.115	-0.080
ethanol	-0.100	-0.071
MEG	-0.085	-0.040
DEG	-0.130	0
TEG	-0.185	0
glycerol	-0.050	0

For methanol, ethanol and MEG there was a need to introduce a binary interaction parameter for the volume of association to describe simultaneously SLE and VLE. The value of the volume of association for water is 0.483 x 10^{-2}, which is just one order of magnitude above the values

presented for the binary interaction parameters, which justifies their relevance for the present equilibria calculations.

For glycerol and diethylene glycol mixtures with water, accurate results were obtained without the need of a β_{ij}. For triethylene glycol mixtures with water, the binary interaction parameters were fitted to the VLE data from Chouireb et al. [21] and to the hydrate dissociation curves with xenon. This is due to the lack of availability of SLE data for this mixture. Xenon results are usually accurate without the need to fit a binary interaction parameter between water and xenon (when SLE data is used for water + other hydrate inhibitors), thus these data were used in place of the SLE data. Tables S1 and S2 in the supporting information present the deviations on pressure and composition for water + methanol and water + ethanol.

Results for the freezing point depression of water + MEG, water + glycerol and water + ethanol are presented in Figure 1. It is important to note that these modelling results do not account for the formation of solid complexes.

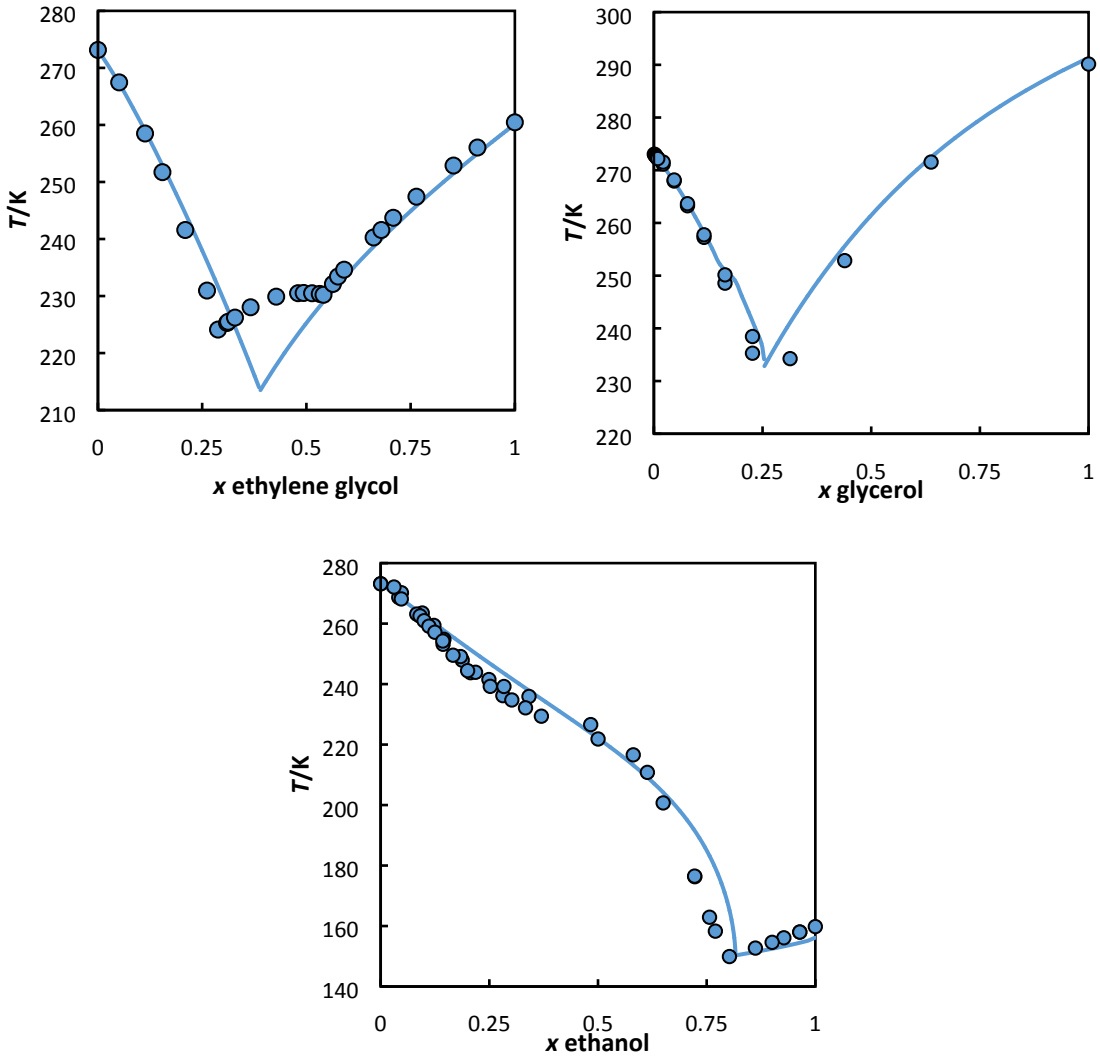

Figure 1 – Freezing point depressions for the mixtures: water + MEG, water + glycerol and water + ethanol. Data taken from the TRC database [22] and Ott *et al*. [23]

The present approach captures the description of most of the ethylene glycol and glycerol SLE diagrams with water. In the case of ethanol it tends to overestimate the ice saturation line.

3.2 Single component gas hydrates

The simplest hydrate inhibition case is that of mixtures of water + hydrate inhibitor + a gas containing a single compound. Starting by compounds known to form hydrates of type I, Figure 2 presents results for mixtures containing methane, water and one inhibitor (methanol, mono ethylene glycol or DEG).

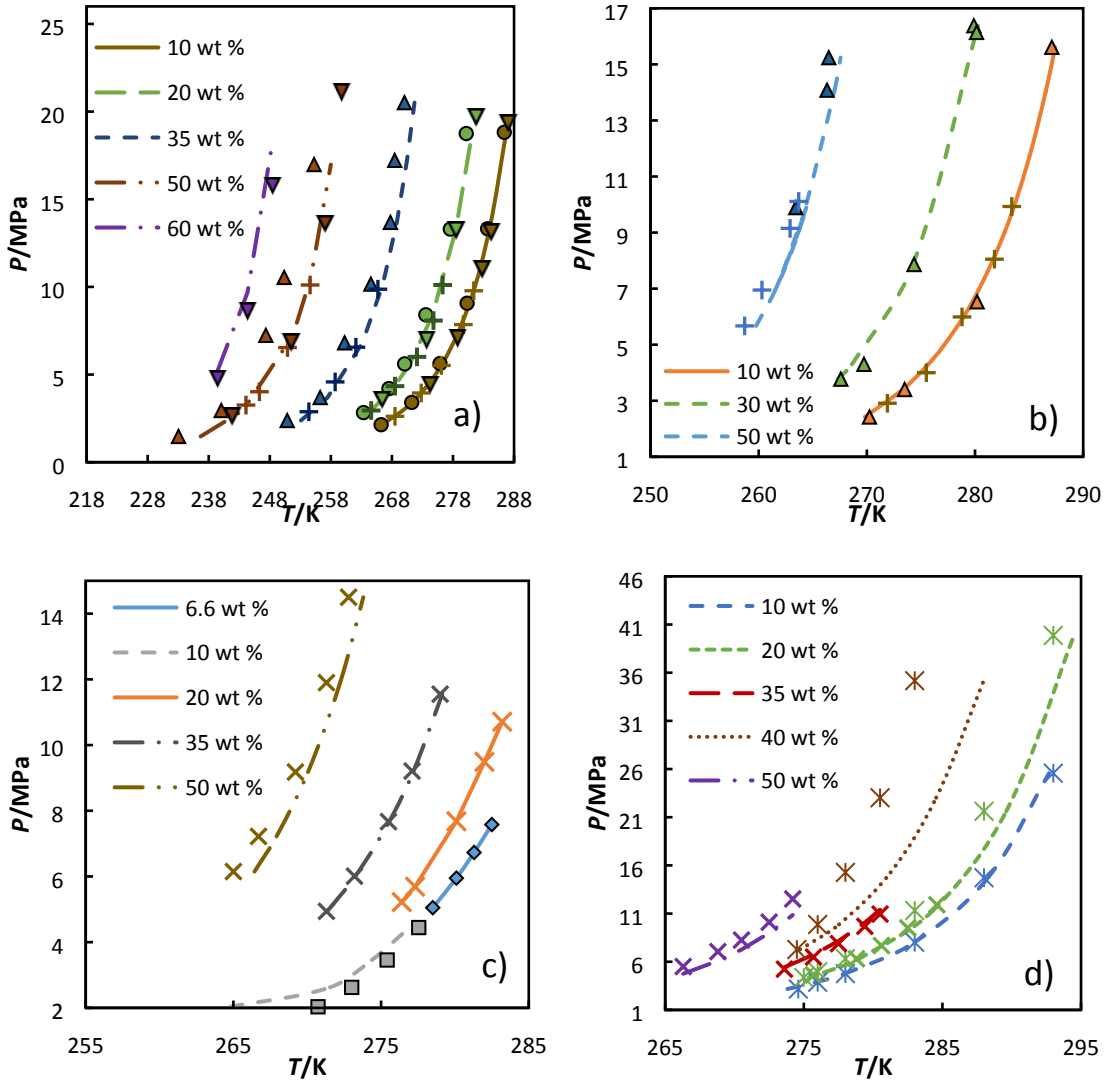

Figure 2 – Hydrate dissociation curves for mixtures of methane + water + inhibitor; Inhibitor a) methanol, b) MEG, c) DEG, d) TEG. wt % refers to weight percentage of inhibitor in aqueous solution. ○ – Ng and Robinson [24]; Δ – Robinson and Ng [25]; x – Mohammadi and Richon [26]; ◊ – Afzal et al. [27]; □ – Mahmoodaghdam and Bishnoi [28]; + – Mohammadi and Richon [29]; * – Ross and Toczylkin. [30]; ∇ - Haghighi et al. [31]

For the mixtures containing methanol, MEG and DEG, the modified CPA is capable of an accurate description of the effect of inhibitor concentration up to 50 wt % (up to 60 % in the case of methanol). There are some uncertainties for the mixture containing 50% of methanol, where the two sets of experimental data differ, with the present approach being able to describe one of the sets. Due to this, the deviations for the inhibition with methanol can reach up to 1.9 K. In the case of diethylene glycol, the results at low pressures present higher deviations, due to the

slower growth of pressure with temperature at these conditions, which leads to a very significant ΔT of around 6.5 K at the data point for the lowest pressure. For the case of TEG the dissociation curves at lower compositions are well described by the model. At higher compositions the data from the different authors are not consistent, with the present model presenting good results when compared to the data of Mohammadi and Richon [26]. The results presented on Table 3 use the complete sets of data from the literature, thus the average deviations obtained consider more data than the one presented on the Figures. Results for methane hydrates in presence of ethanol and glycerol are also presented on Table 3 (as well as on the supporting information).

Most xenon hydrates are correctly described, only considering binary interaction parameters obtained from SLE, between water and the hydrate inhibitor. Figure 3 presents results for the hydrate inhibition of xenon in presence of methanol and TEG. For the cases with the remaining inhibitors results are reported in Table 3 and the supporting information.

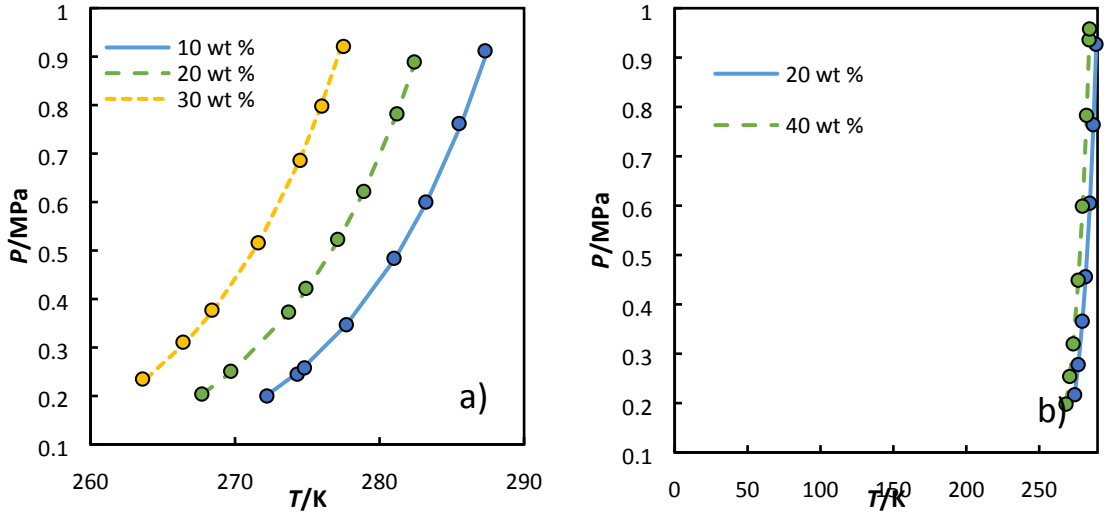

Figure 3 – Hydrate dissociation curves for mixtures of xenon + water + inhibitor; Inhibitor a) methanol, b) TEG. wt % refers to weight percentage of inhibitor in the aqueous phase. ○ – Maekawa. [32]

The results for xenon hydrates are accurate for all cases in analysis.

To continue this analysis with hydrate type I formers, Figure 4 and 5 present results for dissociation curves containing ethane hydrates.

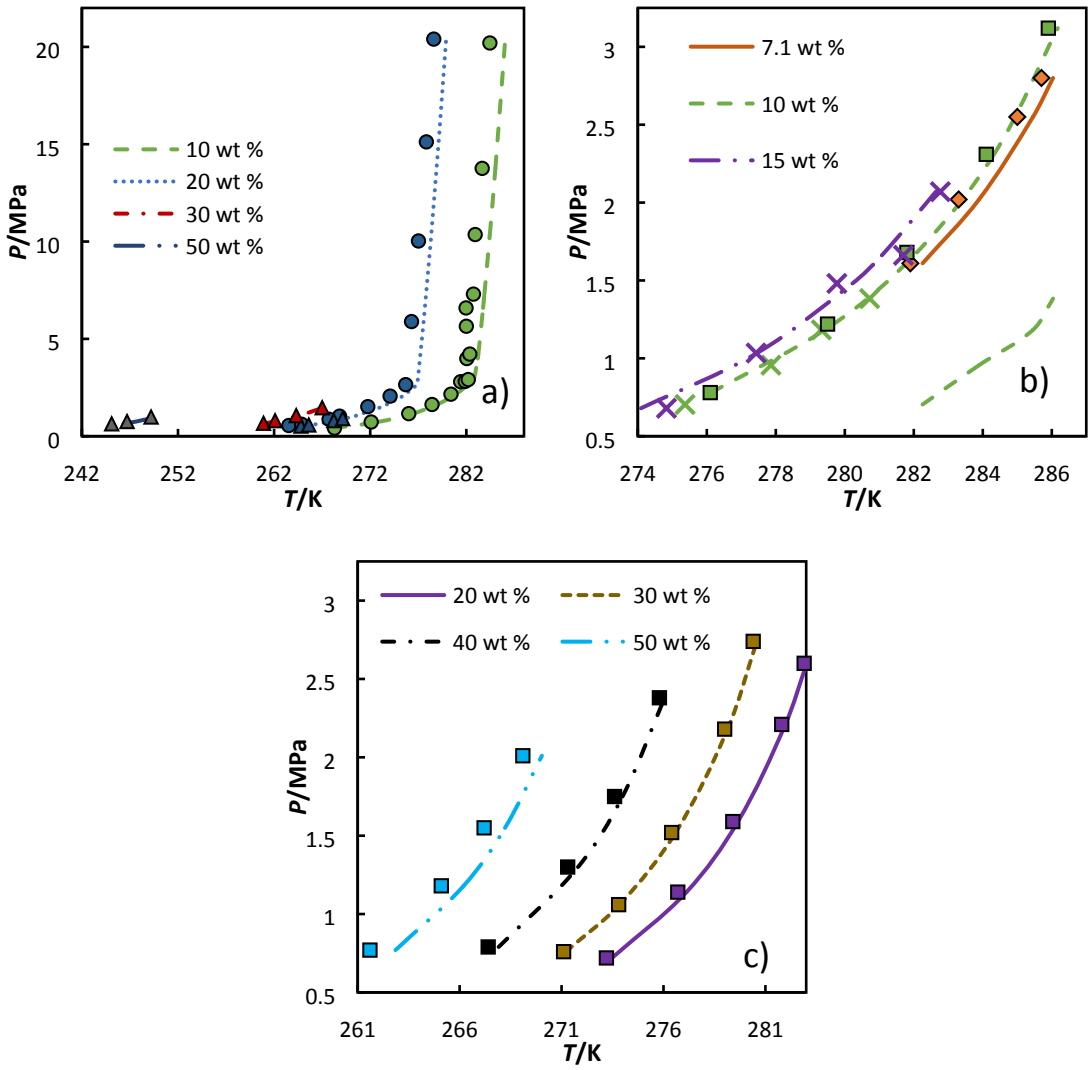

Figure 4 – Hydrate dissociation curves for mixtures of ethane + water + inhibitor; Inhibitor a) methanol, b), c) DEG. wt % refers to weight percentage of inhibitor in the aqueous phase. ○ – Ng and Robinson [24]; Δ – Mohammadi et al. [33]; □ – Maekawa [34]; ◊ – Mahmoodaghdam and Bishnoi [28]; x – Afzal et al. [27].

A very accurate description is obtained for the hydrate dissociation curves of ethane, when inhibited with methanol or DEG, as is presented in Figure 4. In the case of the inhibition with methanol, the model captures the water-liquid-hydrate transition and is able to describe this section of the diagram with a maximum ΔT of 1.9 K. For the case of DEG the deviations are always below 1.25 K. For MEG, TEG and glycerol similar results were obtained and are presented on Figure 5.

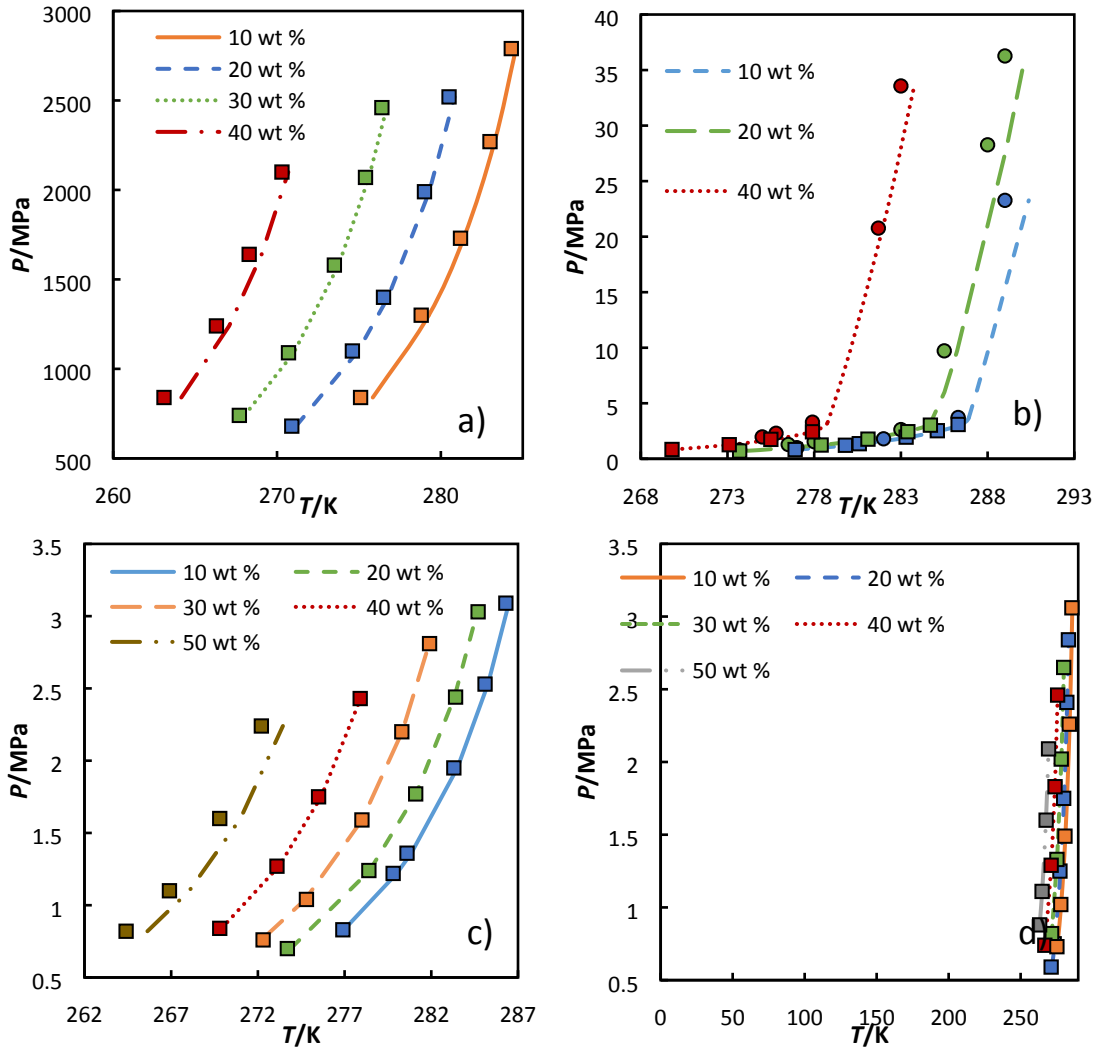

Figure 5 – Hydrate dissociation curves for mixtures of ethane + water + inhibitor; Inhibitor a) MEG b), c) TEG, d) glycerol. wt % refers to weight percentage of inhibitor in aqueous solution. ○ – Ross and Toczylkin [30]; □ – Maekawa. [34]

As in the case of the ethane hydrate inhibition with methanol, the model is able to describe the water-liquid-hydrate section of the diagram for the inhibition with TEG. For the remaining compounds a very accurate description of the water-gas-hydrate section of the dissociation curves is obtained.

For mixtures containing propane, a hydrate type II former, the results are presented on Figures 6 and 7.

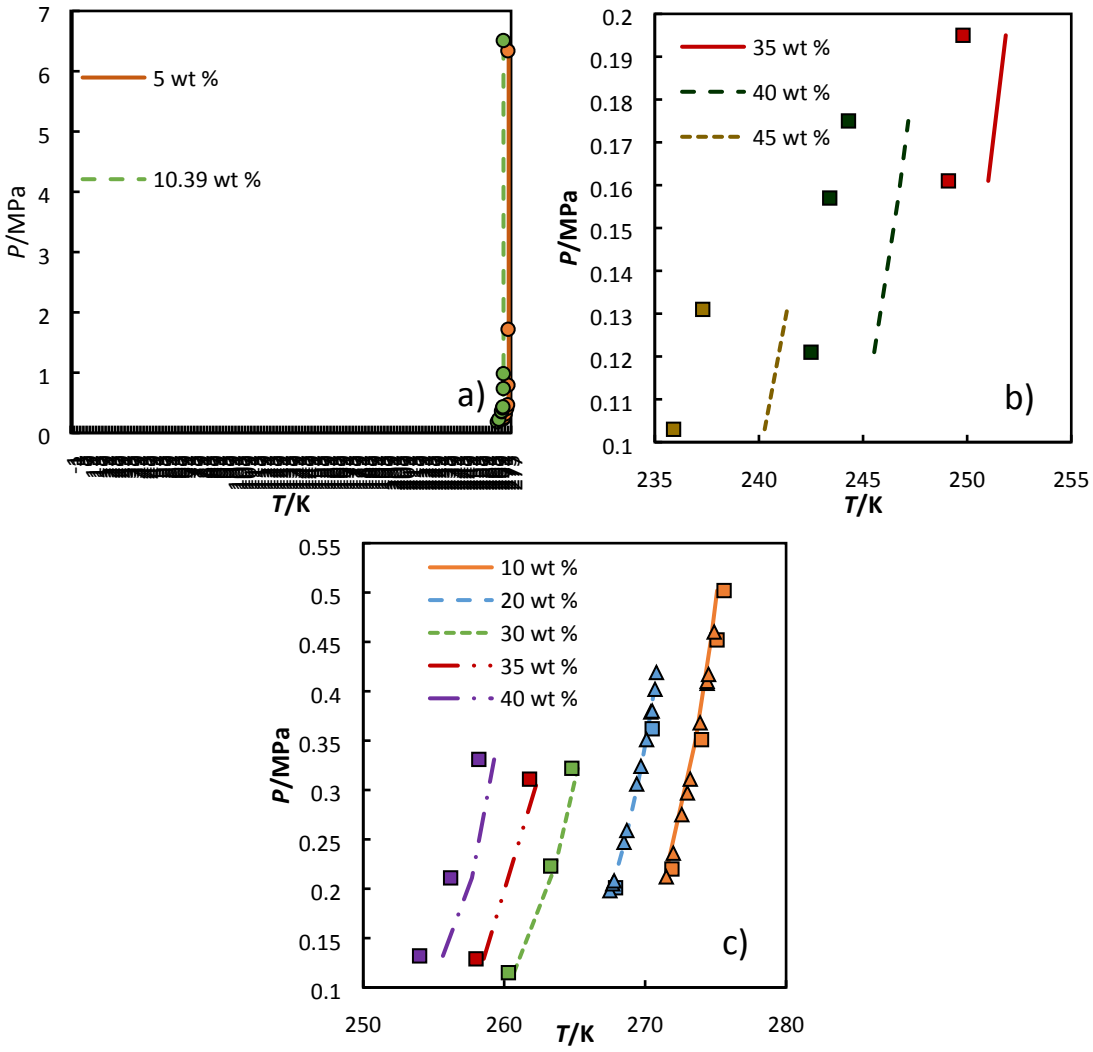

Figure 6 – Hydrate dissociation curves for mixtures of propane + water + inhibitor; Inhibitor a), b) methanol c) MEG. wt % refers to weight percentage of inhibitor in aqueous solution. ○ – Ng and Robinson [24]; □ – Mohammadi and Richon [33]; Δ – Maekawa. [35]

Results for these hydrate dissociation curves are typically accurate, in most cases. For mixtures containing methanol, the results present higher deviations for concentration of hydrate inhibitor above 30 wt %. For the mixture containing MEG the results present a ΔT below 1 K up to 35 wt%.

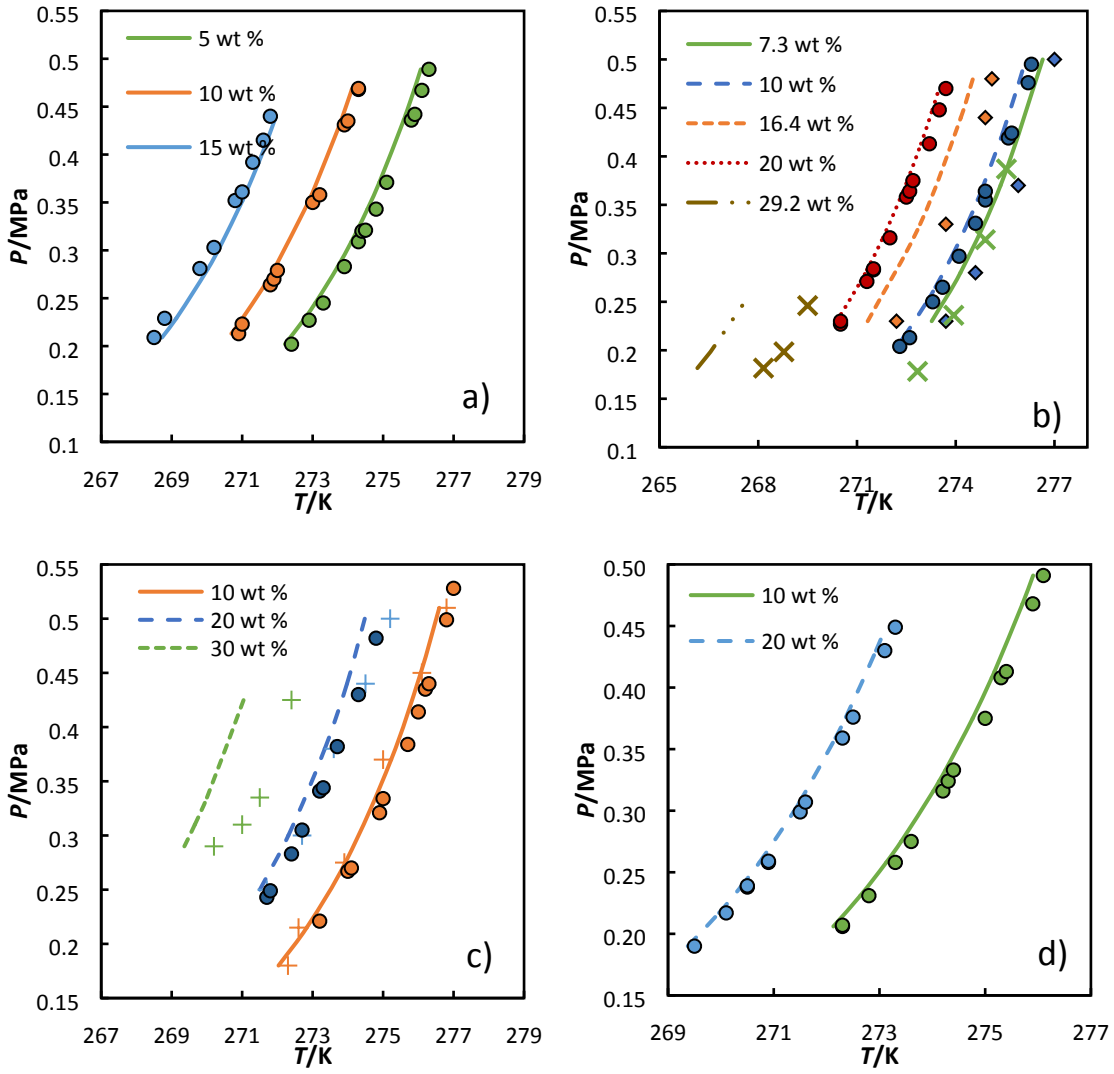

Figure 7 – Hydrate dissociation curves for mixtures of propane + water + inhibitor; Inhibitor a) ethanol, b) DEG, c) TEG, d) glycerol. wt % refers to weight percentage of inhibitor in aqueous solution. ○ – Maekawa. [35]; ◊ -Afzal et al. [27]; x - Mahmoodaghdam and Bishnoi. [28]; + - Servio and Englezos. [36]

For the TEG inhibition, there is an overestimation of the pressure effect for higher inhibition compositions, leading to deviations up to 1.5 K. In the case of diethylene glycol, the results from the different authors are not in accordance with each other, thus, while the model is accurate for certain sets of experimental data, for the data of other authors the deviations may be higher.

To finish the analysis of mixtures containing a single hydrate former, Figure 8 presents the results for the dissociation curves of H_2S, while Figure 9 presents the results for mixtures containing CO_2 hydrates.

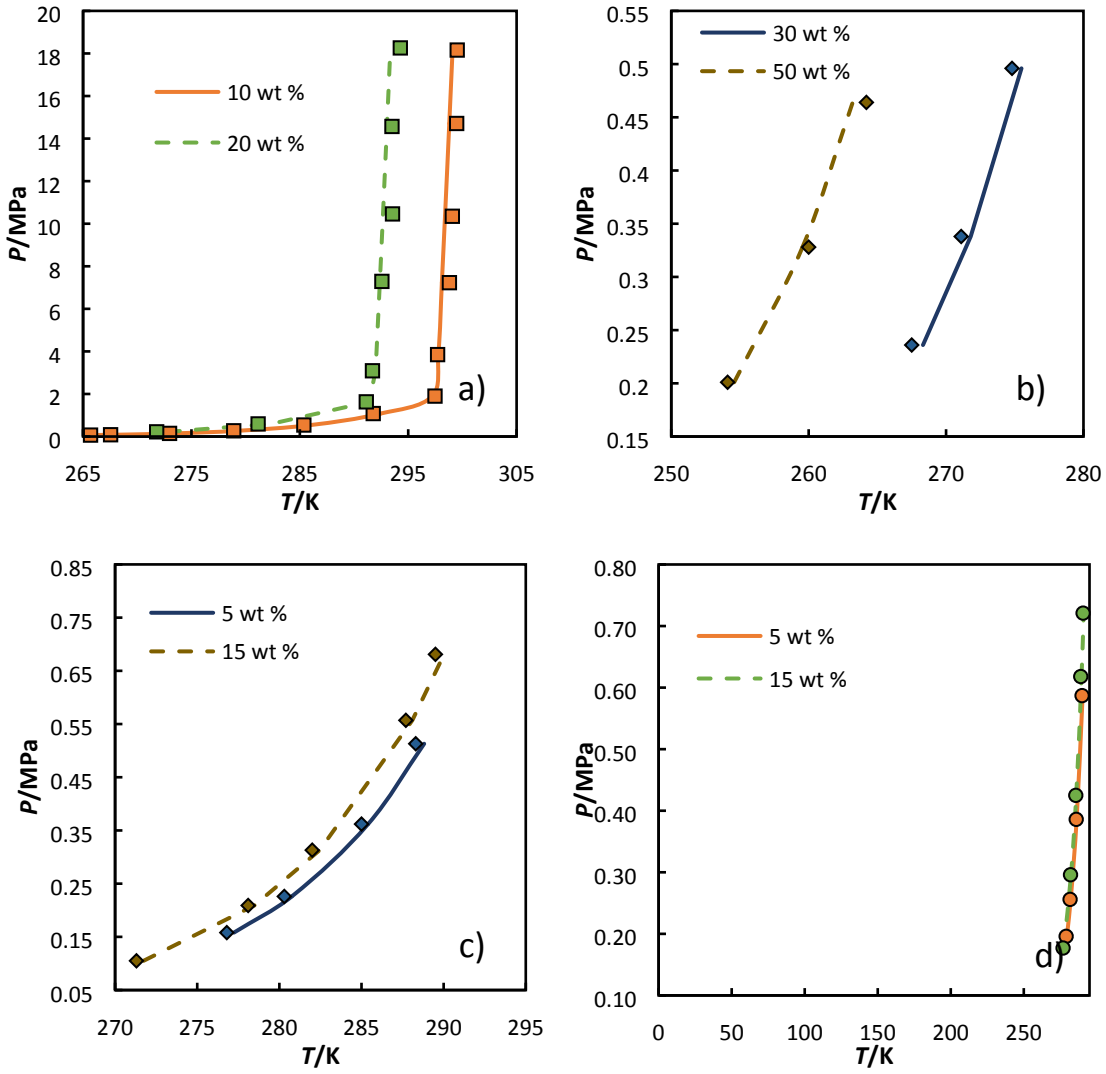

Figure 8 – Hydrate dissociation curves for mixtures of H_2S + water + inhibitor; Inhibitor a), b) methanol, c) DEG, d) TEG. wt % refers to weight percentage of inhibitor in aqueous solution. ○ – Mohammadi and Richon [37]; □ – Ng and Robinson [24]; ◊ – Mohammadi and Richon. [38]

The dissociation curves of H_2S hydrates are accurately described, even at large inhibitor concentrations, in mixtures containing methanol. For the cases of DEG and TEG the results are accurate, in contrast with what happened for propane hydrates. This might have to do with the difference of hydrate type (type I for H_2S and type II for propane), the inhibitor effect of DEG and TEG being better described for hydrates of type I.

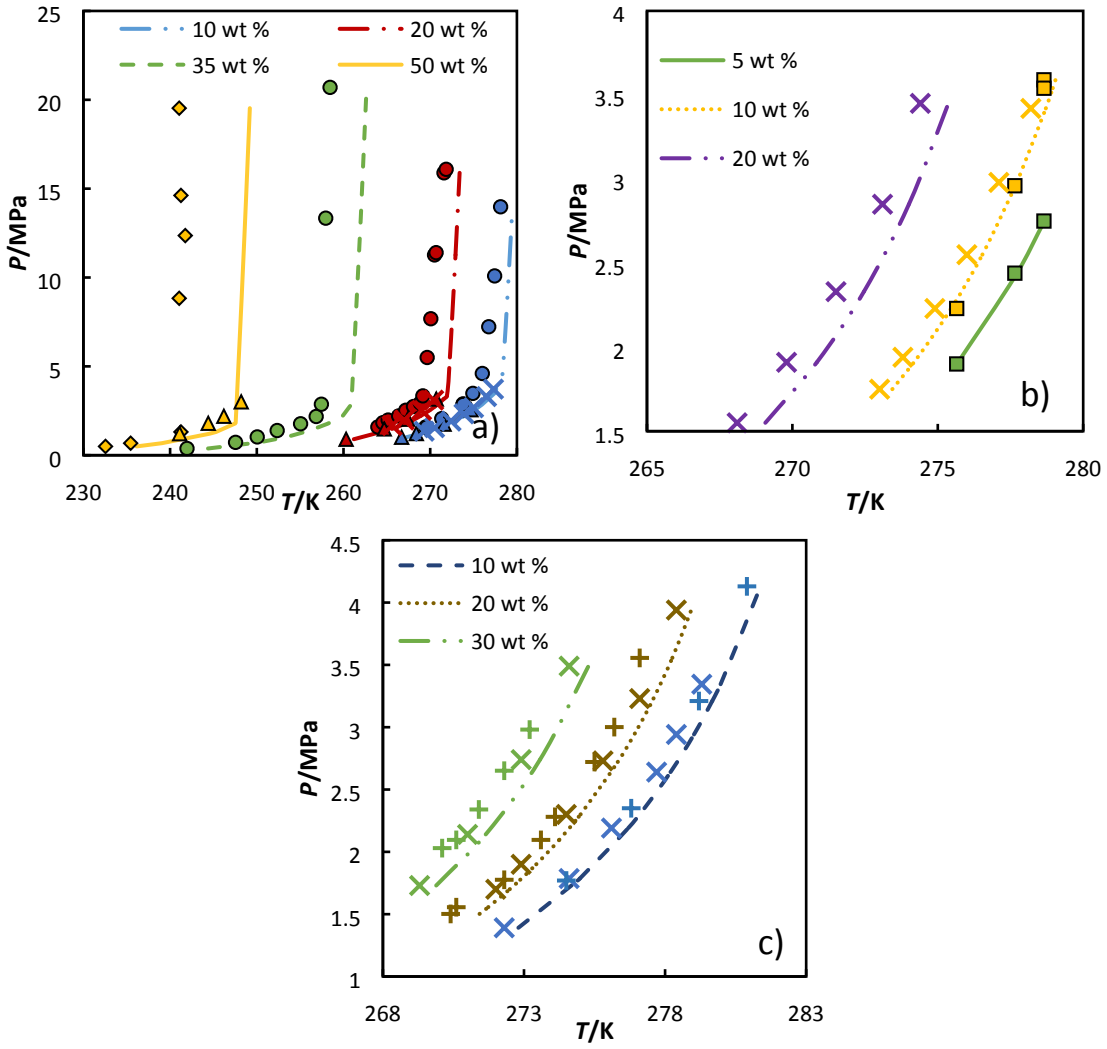

Figure 9 – Hydrate dissociation curves for mixtures of CO_2 + water + inhibitor; Inhibitor a) methanol, b) ethanol, c) glycerol. wt % refers to weight percentage of inhibitor in aqueous solution. ○ – Robinson and Ng [25]; ◊ – Ng and Robbinson [24]; – Δ Mohammadi and Richon [38]; □ – Ferrari et al. [39]; x – Maekawa [40]; + – Breland and Englezos. [41]

For CO_2 (Figure 9), as in some previous cases, the accuracy of the hydrate dissociation curve for mixtures containing methanol depends largely on which set of experimental data is being analyzed. In this case there is a significant difference between the experimental sets, with differences up to 6 K between two sets for the same inhibitor composition. The model describes accurately the results of Mohammadi and Richon [38] and Maekawa [40] at lower inhibitor contents, but clearly underpredicts the pressure results for the remaining sets, especially in the water-liquid-hydrate section of the dissociation curve. As presented in a previous study [20] these differences are already significant for the pure hydrate of CO_2, introducing higher uncertainties for the parameterization of this hydrate. For the remaining compounds in study there appear to be slight underestimations of the hydrate dissociation curves, however, these are within a small range of temperatures and ΔT are mostly below 1 K. Results for the remaining inhibitors in study when applied to the CO_2 hydrate are presented on Table 3 and on the supporting information.

3.3 Mixtures of hydrate formers

In this section, six different gas mixtures are analyzed in presence of hydrate inhibitors. The compositions of these mixtures are presented on Table S3 of the supporting information. Mixture 1 contains methane and ethane. The results for this mixture in contact with water + glycerol and water + TEG solutions are presented in Figure 10.

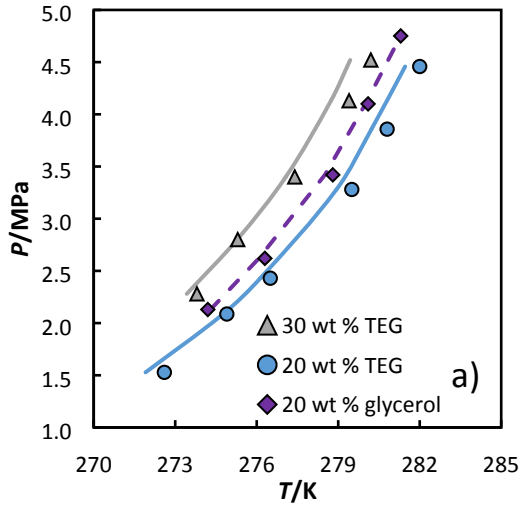

Figure 10 – Hydrate dissociation curves for mixtures of water + inhibitor + methane + ethane. Full lines – results for TEG; Dashed lines – results for glycerol. Data from Wu and Englezos. [42]

The description of the mixture containing ethane is very good at the concentrations of inhibitor in analysis.

Figure 11 compares the results obtained with the modified CPA with the experimental data from Lee and Kang, [43] for natural gas hydrate inhibition.

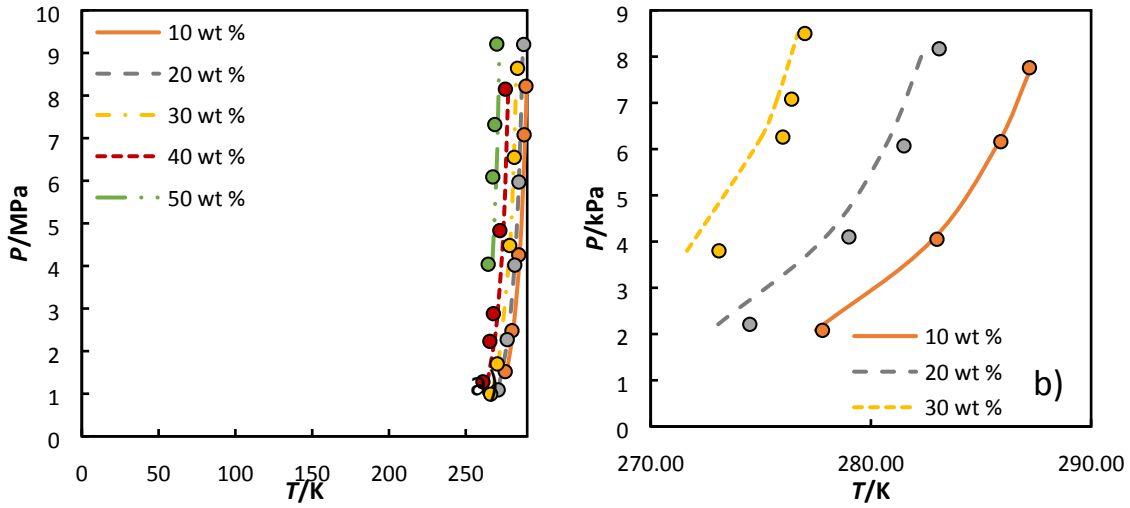

Figure 11 – Hydrate dissociation curves for mixtures of water + natural gas + inhibitor; Inhibitor a) MEG, b) methanol. wt % refers to weight percentage of inhibitor in the aqueous phase. Data from Lee and Kang. [43] (experimental composition data for this mixture is presented in the supporting information)

For the mixture containing MEG, the descriptions are accurate up to 30 wt % of inhibitor with a higher ΔT above these concentrations. In the mixture containing methanol the results are also accurate up to 30 wt% of inhibitor, however, there is no experimental data above this concentration. For both cases ΔT is mostly below 2.0 K.

The last three mixtures being considered in this work are three sour gases + water + methanol. These are analyzed in Figure 12.

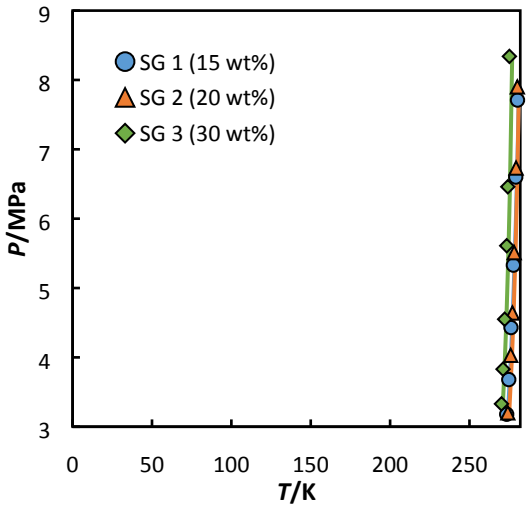

Figure 12 – Hydrate dissociation curves for mixtures of water + sour gas + methanol. wt % refers to weight percentage of methanol in aqueous solution. SG is sour gas. Data from Liu et al. [44] (experimental composition data for these mixtures are presented in the supporting information)

The results obtained for the sour gases present an overestimation of the dissociation temperatures, which for the first two sour gases is mostly below 1 K. For the third sour gas in analysis the deviations can be as high as 1.8 K.

To finish this analysis, Table 3 presents the average ΔT for all mixtures investigated and compares the present results with the results obtained through the Multiflash [10] hydrates model, which also uses a CPA variant (Multiflash 6.1 was used for these calculations). The results from the present work, while, in most cases, not as accurate as the results by Multiflash are still quite good. The parameterization applied in this work tried to improve the description of VLE while keeping a correct description of the hydrate phase. For this purpose, in the cases of methanol, ethanol and MEG, there was a need to use two binary interaction parameters. The Multiflash parameter sets are also capable of a good simultaneous description of hydrate inhibition, SLE and VLE, but the CPA model used in this software, requires a higher number of both pure component and binary interaction parameters. To test the thermodynamic consistency of the results obtained by the model, as well as that of the experimental data, the recent approach presented by Sa et al. [45] can be used. The first of these tests consists in a verification of the linearity of the phase equilibrium data in relation to a fitting regression correlating $\ln P$ to $\frac{1}{T}$. The second test analysis the values of the hydrate dissociation enthalpy, which should only depend on the hydrate structure and on the presence of guest species. The third and last test checks the thermodynamic consistency of the activity of liquid water over a small temperature range. More details on this methods are present on the original paper. [45]

However, it important to note that one of the tests applied in this approach can affected by the phase transition between hydrate and ice and the condensation of heavier alkanes and CO_2. Table 4 presents the results obtained using this approach for the methane hydrate in the presence of high concentrations of inhibitor.

The results for tests 1 and 3 are mostly good, with the model being more consistent than the experimental data in both of these tests. Due to the high inhibitor concentrations, a small change in temperature promotes a large range in the dissociation pressure. Thus for the pure hydrate, the range of temperatures to analyze will be large, which affects negatively the results, especially for the second test. Thus, in general, the present results seem to be thermodynamically consistent.

Conclusions

A modified CPA model was applied in combination with the van der Waals-Platteeuw hydrate model for the description of hydrate dissociation curves of inhibited mixtures. For most mixtures the descriptions of the experimental data are quite good and the average differences are in all cases below 2 K.

The parameterization conducted for methanol, ethanol and ethylene glycol took into account the description of SLE and a large range of VLE data. Thus, one extra binary interaction parameter was needed to enable a correct overall description of phase equilibria. This approach leads to higher deviations, especially at higher inhibitor compositions, but this is a necessary compromise for a model capable of describing the different equilibria without a high number of binary interaction parameters.

When compared to the CPA model present on Multiflash, the proposed approach compares well on the deviations in temperature for the dissociation curves. Nevertheless, the model present in Multiflash is capable of describing a broader range of phase equilibria with a single set of parameters. This is, however, due to a higher number of parameters used by this model.

Supporting information

Deviations on pressure and composition for the Vapor Liquid Equilibria of water + methanol and water + ethanol. Figures with some extra results for hydrate inhibition. Experimental composition of the sour and natural gas mixtures.

Funding and Acknowledgments

This work was funded by KBC Advanced Technologies Limited (A Yokogawa Company) under project "Extension of the CPA model for Polyfunctional Associating Mixtures". André M. Palma Acknowledges KBC for his Post-Doctoral grant. This work was developed within the scope of the project CICECO-Aveiro Institute of Materials, FCT Ref. UID/CTM/50011/2019, financed by national funds through the FCT/MCTES.

Table 3 – Differences in hydrate dissociation temperature between experiment and model for the presented model and the CPA hydrate model present in Multiflash (version 6.1). [10]

Gas/references	*ΔT (K)*										
	methanol		**MEG**		**ethanol**		**DEG**		**TEG**		**glycerol**
	This work	MFlash	This work	MFlash	This work	MFlash	This work	MFlash	This work	MFlash	This work
methane[24–30,46–48]	0.82	0.78	0.49	0.53	0.43	0.22	0.71	1.66	0.98	1.31	0.82
ethane[24,27,28,30,33,34]	0.94	0.78	0.41	0.20	-	-	0.35	0.82	0.64	1.35	0.20
propane[24,27,28,30,33,35]	1.03	0.53	0.44	0.46	0.19	0.49	0.59	1.08	0.41	0.17	0.16
Xe[32]	0.10	0.24	0.17	0.33	0.31	0.34	0.31	1.35	0.14	1.20	0.21
H_2S[24,37,38]	0.59	0.50	-	-	-	-	0.44	0.41	0.40	0.48	-
CO_2[25,38–41]	2.17	1.43	0.73	0.25	0.43	0.16	0.70	0.40	0.41	0.75	0.67
CH_4+C_2H_6[42]	-	-	-	-	-	-	-	-	0.44	0.29	0.16
natural gas[43]	0.67	0.90	1.18	0.92	-	-	-	-	-	-	-

sour gas[44]	0.94	0.75	-	-	-	-	-	-	-	-	-

Table 4 – Results for the thermodynamic consistency test of Sa et al for methane hydrates. [45]

Inhibitor	Reference	EXP			CALC		
		Test 1	Test 2	Test 3	Test 1	Test 2	Test 3
methanol (40%)	31	Good	Average	Average	Good	Good	Good
methanol (50%)	31	Good	Bad	Good	Good	Average	Good
methanol (60%)	31	Good	Average	Good	Good	Average	Good
methanol (50%)	25	Good	Bad	Average	Good	Bad	Average
methanol (50%)	29	Good	Bad	Good	Good	Bad	Good
MEG (50%)	25	Good	Bad	Good	Good	Bad	Good
MEG (50%)	29	Good	Good	Good	Good	Good	Good
DEG (50%)	26	Good	Good	Good	Good	Average	Good
TEG (40%)	30	Good	Bad	Average	Good	Bad	Good
TEG (50%)	26	Good	Average	Good	Good	Good	Good

Nomenclature

A, a = energy parameter of CPA. ($A(T) = n^2 a(T)$)

a_c = value of the energy parameter at the critical point.

B, b = co-volume. ($B = nb$)

$c_1 - c_5$ (c_x)= alpha function parameters

c_{vs} = volume shift

g = radial distribution function

k_{ij} = binary interaction parameter for the cubic term energy parameter

m_i = mole number of sites of type *i*

n = mole number

P = Pressure (Pa)

R = Gas constant

T = temperature (K)

T_r = reduced temperature $T_r = \frac{T}{T_c}$

T'= $(1 - \sqrt{T_r})$, $T_r = T/T_c$

v = molar volume ($m^3.mol^{-1}$)

v_0 = molar volume before translation ($m^3.mol^{-1}$)

v_t = molar volume after translation ($m^3.mol^{-1}$)

wt % = weight percentage

x = mole fraction

X_{A_i} = mole fraction of component *i* not bonded to site A

Z = compressibility factor

Subscripts and superscripts

c = critical

exp = experimental

calc = calculated

Chemical Formulas

CO_2 = carbon dioxide

H_2S = hydrogen sulfide

Abbreviations

CPA EoS = Cubic Plus Association Equation of State

DEG = diethylene glycol

MEG = ethylene glycol

OF = Objective Function

PC-SAFT = Perturbed Chain SAFT

SAFT = Statistical Associating Fluid Theory

SAFT-VR = SAFT Variable Range

SG = Sour gas

TEG = triethylene glycol

References

(1) Platteeuw, J. C.; van der Waals, J. H. Thermodynamic properties of gas hydrates. *Mol. Phys. An Int. J. Interface Between Chem. Phys.* **1958**, No. June 2013, 91–96.

(2) Parrish, W. R.; Prausnitz, J. M. Dissociation Pressures of Gas Hydrates Formed by Gas Mixtures. *Ind. Eng. Chem. Process Des. Dev.* **1972**, *11* (1), 26–35.

(3) Dadmohammadi, Y.; Gebreyohannes, S.; Abudour, A. M.; Neely, B. J.; Gasem, K. A. M. Representation and Prediction of Vapor-Liquid Equilibrium Using the Peng-Robinson Equation of State and UNIQUAC Activity Coefficient Model. *Ind. Eng. Chem. Res.* **2016**, *55* (4), 1088–1101.

(4) Palma, A. M.; Oliveira, M. B.; Queimada, A. J.; Coutinho, J. A. P. Re-evaluating the CPA EoS for improving critical points and derivative properties description. *Fluid Phase Equilib.* **2017**, *436*, 85–97.

(5) Folas, G. K.; Froyna, E. W.; Lovland, J.; Kontogeorgis, G. M.; Solbraa, E. Data and prediction of water content of high pressure nitrogen, methane and natural gas. *Fluid Phase Equilib.* **2007**, *252* (1–2), 162–174.

(6) Pedrosa, N.; Szczepanski, R.; Zhang, X. Integrated equation of state modelling for flow assurance. *Fluid Phase Equilib.* **2013**, *359*, 24–37.

(7) Li, X. Sen; Wu, H. J.; Englezos, P. Prediction of gas hydrate formation conditions in the presence of methanol, glycerol, ethylene glycol, and triethylene glycol with the statistical associating fluid theory equation of state. *Ind. Eng. Chem. Res.* **2006**, *45* (6), 2131–2137.

(8) Dufal, S.; Galindo, A.; Jackson, G.; Haslam, A. J. Modelling the effect of methanol, glycol inhibitors and electrolytes on the equilibrium stability of hydrates with the SAFT-VR approach. *Mol. Phys.* **2012**, *110* (11–12), 1223–1240.

(9) Kondori, J.; Zendehboudi, S.; James, L. A.; James, L. Evaluation of Gas Hydrate Formation Temperature for Gas/Water/Salt/Alcohol Systems: Utilization of Extended UNIQUAC Model and PC-SAFT Equation of State. *Ind. Eng. Chem. Res.* **2018**, *57*, 13833–13855.

(10) MULTIFLASH version 6.1, KBC Process Technology, London, United Kingdom.

(11) Kontogeorgis, G. M.; Yakoumis, I. V.; Meijer, H.; Hendriks, E.; Moorwood, T. Multicomponent phase equilibrium calculations for water–methanol–alkane mixtures. *Fluid Phase Equilib.* **1999**, *160*, 201–209.

(12) Palma, A. M.; Queimada, A. J.; Coutinho, J. A. P. Improved prediction of water properties and phase equilibria with a modified CPA EoS. *Ind. Eng. Chem. Res.* **2017**, *56*, 15163−15176.

(13) Elliott, J. R.; Suresh, S. J.; Donohue, M. D. A Simple Equation of State for Nonspherical and Associating Molecules. *Ind. Eng. Chem. Res.* **1990**, *32* (1978), 1476–1485.

(14) Voutsas, E. C.; Yakoumis, I. V; Tassios, D. P. Prediction of phase equilibria in water/alcohol/alkane systems. *Fluid Phase Equilib.* **1999**, *158–160*, 151–163.

(15) Kontogeorgis, G. M.; Michelsen, M. L.; Folas, G. K.; Derawi, S.; Von Solms, N.; Stenby, E. H. Ten Years with the CPA (Cubic-Plus-Association) equation of state. Part 2. Cross-Associating and Multicomponent Systems. *Ind. Eng. Chem. Res.* **2006**, *45* (14), 4855–4868.

(16) Palma, A. M.; Queimada, A. J.; Coutinho, J. A. P. Modeling of the Mixture Critical Locus with a Modified Cubic Plus Association Equation of State: Water, Alkanols, Amines, and Alkanes. *Ind. Eng. Chem. Res.* **2018**, acs.iecr.8b01960.

(17) Palma, A. M.; Queimada, A. J.; Coutinho, J. A. P. Modeling of the Mixture Critical Locus with a Modified Cubic Plus Association (CPA) EoS: Aromatics, Ketones, Ethers, Diethyl Carbonate, and THF. *Ind. Eng. Chem. Res.* **2018**, *57* (46), 15857–15868.

(18) Graboski, M. S.; Daubert, T. E. A Modified Soave Equation of State for Phase Equilibrium Calculations. 1. Hydrocarbon Systems. *Ind. Eng. Chem. Process Des. Dev.* **1978**, *17* (4), 443–448.

(19) Palma, A. M.; Oliveira, M. B.; Queimada, A. J.; Coutinho, J. A. P. Evaluating Cubic Plus Association Equation of State Predictive Capacities: A Study on the Transferability of the Hydroxyl Group Associative Parameters. *Ind. Eng. Chem. Res.* **2017**, *56* (24), 7086–7099.

(20) Palma, A. M.; Queimada, A. J.; Coutinho, J. A. P. Modelling of hydrate dissociation curves with a modified Cubic-Plus-Association equation of state. (Under Consideration for Industrial and Engineering Chemistry Research).

(21) Chouireb, N.; Crespo, E. A.; Pereira, L. M. C.; Tafat-Igoudjilene, O.; Vega, L. F.; Coutinho, J. A. P.; Carvalho, P. J. Measurement and Modeling of Isobaric Vapor-Liquid Equilibrium of Water + Glycols. *J. Chem. Eng. Data* **2018**, *63* (7), 2394–2401.

(22) Thermodynamics Research Center (TRC), ThermoData Engine, version 9.0, National Institute of Standards and Technology, Boulder, Colorado, USA.

(23) Ott, J. B.; Goates, J. R.; Lamb, J. D. Solid-liquid phase equilibria in water + ethylene glycol. *J. Chem. Thermodyn.* **1972**, *4* (1), 123–126.

(24) Ng, H.-J.; Robinson, D. B. Hydrate formation in systems containing methane, ethane, propane, carbon dioxide or hydrogen sulfide in the presence of methanol. *Fluid Phase Equilib.* **1985**, *21* (1–2), 145–155.

(25) Robinson, D. B.; Ng, H. J. Hydrate Formation and Inhibition in Gas or Gas Condensate Streams. *J. Can. Pet. Technol.* **1986**, *25* (4), 26–30.

(26) Mohammadi, A. H.; Richon, D. Gas hydrate phase equilibrium in methane + ethylene glycol, diethylene glycol, or triethylene glycol + water system. *J. Chem. Eng. Data* **2011**,

56 (12), 4544–4548.

(27) Afzal, W.; Mohammadi, A. H.; Richon, D. Experimental Measurements and Predictions of Dissociation Conditions for Methane, Ethane, Propane, and Carbon Dioxide Simple Hydrates in the Presence of Diethylene Glycol Aqueous Solutions. *J. Chem. Eng. Data* **2008**, *53* (3), 663–666.

(28) Mahmoodaghdam, E.; Bishnoi, P. R. Equilibrium Data for Methane, Ethane, and Propane Incipient Hydrate Formation in Aqueous Solutions of Ethylene Glycol and Diethylene Glycol. *J. Chem. Eng. Data* **2002**, *47* (2), 278–281.

(29) Mohammadi, A. H.; Richon, D. Phase Equilibria of Methane Hydrates in the Presence of Methanol and/or Ethylene Glycol Aqueous Solutions. *Ind. Eng. Chem. Res.* **2010**, *49* (2), 925–928.

(30) Ross, M. J.; Toczylkin, L. S. Hydrate dissociation pressures for methane or ethane in the presence of aqueous solutions of triethylene glycol. *J. Chem. Eng. Data* **1992**, *37* (4), 488–491.

(31) Haghighi, H.; Chapoy, A.; Burgess, R.; Mazloum, S.; Tohidi, B. Phase equilibria for petroleum reservoir fluids containing water and aqueous methanol solutions: Experimental measurements and modelling using the CPA equation of state. *Fluid Phase Equilib.* **2009**, *278* (1–2), 109–116.

(32) Maekawa, T. Equilibrium Conditions of Xenon Hydrates in the Presence of Aqueous Solutions of Alcohols, Glycols, and Glycerol. *J. Chem. Eng. Data* **2016**, *61* (1), 662–665.

(33) Mohammadi, A. H.; Richon, D. Phase equilibria of propane and ethane simple hydrates in the presence of methanol or ethylene glycol aqueous solutions. *Ind. Eng. Chem. Res.* **2012**, *51* (6), 2804–2807.

(34) Maekawa, T. Equilibrium Conditions of Ethane Hydrates in the Presence of Aqueous Solutions of Alcohols, Glycols, and Glycerol. *J. Chem. Eng. Data* **2012**, *57* (2), 526–531.

(35) Maekawa, T. Equilibrium conditions of propane hydrates in aqueous solutions of alcohols, glycols, and glycerol. *J. Chem. Eng. Data* **2008**, *53* (12), 2838–2843.

(36) Servio, P.; Englezos, P. Incipient equilibrium propane hydrate formation conditions in aqueous triethylene glycol solutions. *J. Chem. Eng. Data* **1997**, *42* (4), 800–801.

(37) Mohammadi, A. H.; Richon, D. Phase Equilibria of Clathrate Hydrates in Hydrogen Sulfide + Diethylene Glycol or Triethylene Glycol + Water System. *Chem. Eng. Commun.* **2014**, *201* (2), 225–232.

(38) Mohammadi, A. H.; Richon, D. Phase equilibria of hydrogen sulfide and carbon dioxide simple hydrates in the presence of methanol, (methanol + NaCl) and (ethylene glycol + NaCl) aqueous solutions. *J. Chem. Thermodyn.* **2012**, *44* (1), 26–30.

(39) Ferrari, P. F.; Guembaroski, A. Z.; Marcelino Neto, M. A.; Morales, R. E. M.; Sum, A. K. Experimental measurements and modelling of carbon dioxide hydrate phase equilibrium with and without ethanol. *Fluid Phase Equilib.* **2016**, *413*, 176–183.

(40) Maekawa, T. Equilibrium Conditions for Carbon Dioxide Hydrates in the Presence of Aqueous Solutions of Alcohols, Glycols, and Glycerol. *J. Chem. Eng. Data* **2010**, *55* (3), 1280–1284.

(41) Breland, E.; Englezos, P. Equilibrium hydrate formation data for carbon dioxide in aqueous glycerol solutions. *J. Chem. Eng. Data* **1996**, *41* (1), 11–13.

(42) Wu, H.-J.; Englezos, P. Inhibiting Effect of Triethylene Glycol and Glycerol on Gas Hydrate Formation Conditions. *J. Chem. Eng. Data* **2006**, *51*, 1811–1813.

(43) Lee, J. W.; Kang, S. P. Phase equilibria of natural gas hydrates in the presence of methanol, ethylene glycol, and NaCl aqueous solutions. *Ind. Eng. Chem. Res.* **2011**, *50* (14), 8750–8755.

(44) Liu, H.; Guo, P.; Du, J.; Wang, Z.; Chen, G.; Li, Y. Experiments and modeling of hydrate phase equilibrium of CH4/CO2/H2S/N2 quaternary sour gases in distilled water and methanol-water solutions. *Fluid Phase Equilib.* **2017**, *432*, 10–17.

(45) Sa, J. H.; Hu, Y.; Sum, A. K. Assessing thermodynamic consistency of gas hydrates phase equilibrium data for inhibited systems. *Fluid Phase Equilib.* **2018**, *473*, 294–299.

(46) Sloan, E. D.; Koh, C. *Clathrate Hydrates of Natural Gases*; 2007.

(47) Ng., H.-J. .; Robinson, D. B. (First) International Conference on Natural Gas Hydrates. In *Ann. N.Y. Acad. Sci.*; 1994; pp 715, 450.

(48) Youn, Y.; Seol, J.; Cha, M.; Ahn, Y. H.; Lee, H. Structural transition induced by CH4 enclathration and cage expansion with large guest molecules occurring in amine hydrate systems. *J. Chem. Eng. Data* **2014**, *59* (6), 2004–2012.

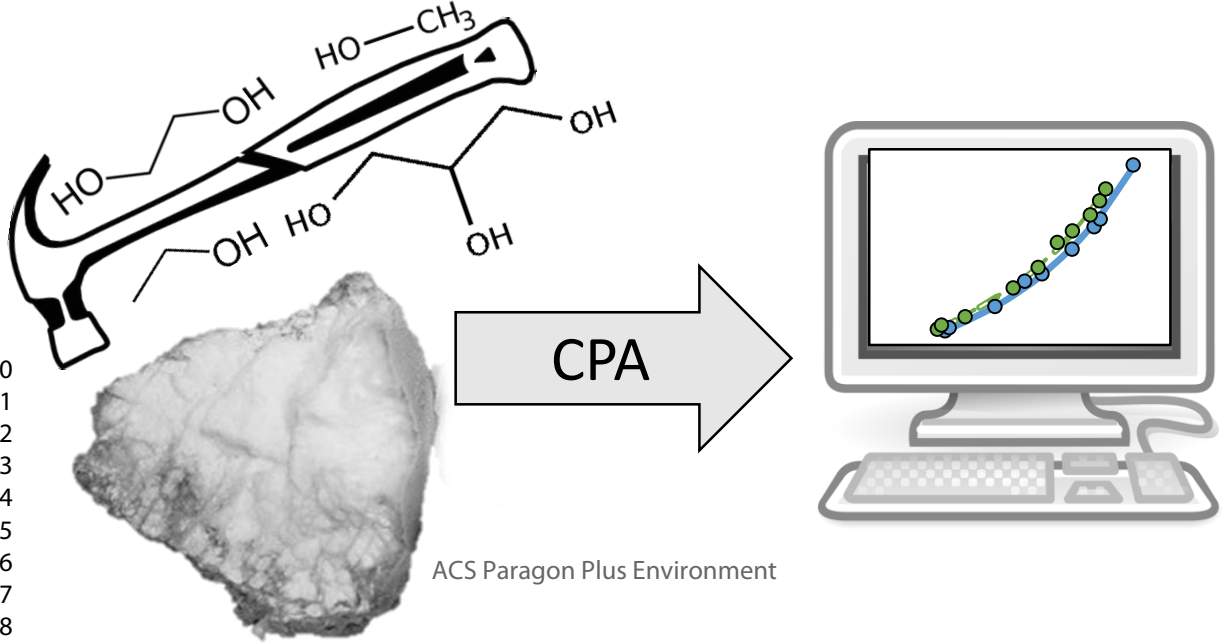

ACS Paragon Plus Environment